Tuning the Electronic Properties of Metal Rich-Borides

Andreas Leithe-Jasper, Helge Rosner, Roman Gumeniuk, Ulrich Burkhardt, Walter Schnelle, Wilder Carrillo-Cabrera, Gudrun Auffermann, Miriam Schmitt, Yuri Prots, Igor Veremchuk, and Yuri Grin

Introduction

The physical properties of transition-metal-rich intermetallic compounds are often governed by the nature of the major constituent. In many cases the crystal structure of these compounds is dominated by units already present in the elemental structures. In fact, already filling up their interstitial sites to certain limits by light and small elements like carbon, nitrogen or boron can be regarded in many cases as an approach towards compound formation which takes place once individual solid solution threshold concentrations are passed.

In all respects, the archetypal metallurgical and technologically most important system represents the iron-rich part of the iron-carbon system. Depending on additional metal alloying partners, temperature, as well as thermal and mechanical history, carbon-stabilized intermetallic phases nucleate, form, precipitate, disperse or dissolve. These alloy micro-constituents play a significant role influencing the properties of cast iron and steels in which they are contained and thus, they have been the topic of structural and thermodynamic investigations ever since the importance of the microstructure of these iron-based alloys has been realized. In the course of a detailed analysis of carbide phases found in stainless steels, *Westgren* [1] recognized already in 1928 that these transition-metal-rich phases by no means have simple stoichiometric proportions and display rather complex atomic arrangements, as it is the case (besides several others) for $M_{23}C_6$ carbides. This class of compounds which derives from the binary cubic compound $Cr_{26}C_6$ [2] shows a wide composition range with respect to constituting metals as well as stabilizing elements.

At the same time it was also recognized in the course of the metallurgical investigations and through advancements of cast iron that additions of non-transition-metals (like Mg, Al, Sn, Zn or rare-earth (*RE*) metals) can induce certain graphite precipitation in rather specific ways. On the other hand, depending on the added metal *A*, detailed analyses revealed the formation of new phases with the composition AT_3C (transition-metal *T*) [3,4]. They crystallize with comparatively simple structures which are compatible with the close packed *fcc* arrangement of metals. As side products in these metallurgical processes they influence in a detrimental way, or even inhibit graphitization. Astonishingly, the peculiar atomic arrangements in these phases can be related to a classical intermetallic structure type, namely the $AuCu_3$ type as well as to oxides, specifically the perovskite $CaTiO_3$. Here, we can think of a quasi anti-arrangement in which the light element (O) and transition metal (Ti) positions are exchanged.

Besides the metallurgical implications these phases also have a history of interest concerning their structural chemistry as well as inherent physical properties. For example, it has been known for a long time that carbon can be completely replaced by boron under equilibrium conditions in both of these compound classes by progressing from the early transition metals to cobalt and nickel. In case of crystal structures of the $Cr_{23}C_6$ type additional stabilizing atomic species have to be accommodated on a special lattice position (see below) [4,5].

In this respect, nickel-based phases have been investigated for possible use as binder materials for refractory and hard boron-rich compounds as well as utilization of their intrinsic hardness for wear-resistant coatings. Furthermore, in these transition-metal metalloid systems the formation of metastable phases and metallic glasses can be observed as function of applied cooling rates [6]. The soft magnetic properties particularly found in ferrous amorphous boron-containing alloys have led to significant applications as electro-magnetic materials. Utilization of partial crystallization of amorphous precursor alloys with appropriate compositions has been found to represent a promising preparation route towards nanocomposites with superior characteristics comprising ultra-small crystalline grains in a residual amorphous matrix. Here, detailed knowledge of the multi-step crystal-

lization processes involved are of significant interest since nucleation of additional phases usually has a detrimental influence on the properties [7]. In many cases, the analysis of such secondary crystallization products revealed the formation of compounds with the $Cr_{23}C_6$ type of structure.

Since many of these multi-component systems contain zirconium and also lanthanide metals, a detailed analysis of the physical properties of possible boundary phases is desirable. For this purpose we have investigated a series of $RE_2Ni_{21}B_6$ compounds [8]. To study the magnetic properties of these nickel-rich phases we have undertaken a joint experimental and theoretical approach. Here, we confined ourselves to compounds with non-magnetic stabilizers *RE* = Y, Lu together with Zr. We also explored the influence of transition-metal additions like Co and Cu on the magnetic properties.

Recently, the $AuCu_3$/anti-perovskite related phases attracted much attention due to discovery of superconductivity in the compound $MgNi_3C$ [10]. This is a rather remarkable behavior since the substantial Ni content can be expected to result in a large and strong competition between magnetic and superconducting electronic ground states [11]. Therefore, intermetallic anti-perovskites which are closely related to $MgNi_3C$ are subject of investigations, both in the search for new superconductors and in the pursuit of better understanding of the interplay between superconductivity and magnetism. To this end, boron-containing anti-perovskites may be good candidates. Therefore, we recently started a concerted theoretical and experimental study [9] in the systems $RePd_3B$. This material contains non-magnetic Pd as transition metal and thus should show less tendency towards ferromagnetism. Moreover, a variety of electronic structures has been found while changing the boron content and the *RE* metal from La to Lu.

Here we would like to demonstrate how the electronic structure can be tuned in these compounds. We have exemplarily chosen one member of each family of these compound classes: $Lu_{2-x}Ni_{21}B_6$ and $EuPd_3B_x$. Our tuning results in band magnetism in $Lu_{2-x}Ni_{21-y}Co_yB_6$ and a valance change of Eu in $EuPd_3B_x$ as a function of boron content. We compare theoretical results with the experimental findings and discuss the challenging task of quantitatively determining the content of the light element boron in these metal-rich compounds.

Ternary Boride $Lu_{2-x}Ni_{21}B_6$

$Lu_{2-x}Ni_{21}B_6$ crystallizes with the $Cr_{23}C_6$ type of structure (space group $Fm\bar{3}m$, Fig.1) [2]. B atoms occupy the 24*(e)* position of C atoms, while Ni atoms are situated in the three crystallographic sites (Cr1 on 4*(a)*, Cr2 on 32*(f)* and Cr3 on 48*(h)*) that are occupied by Cr atoms in the prototype. In ternary $Lu_{2-x}Ni_{21}B_6$, a partial occupancy of the 8*(c)* position (occupied by a Cr atom in the binary prototype) by the structure-stabilizing element Lu is observed. Refinement of single crystal X-ray diffraction data and wave-length dispersive X-ray spectroscopy (WDXS) analysis gave a composition $Lu_{1.65}Ni_{21}B_6$.

The polyhedra of Ni atoms form columns consisting of tetragonal antiprisms [$BNi2_4Ni3_4$] (filled by B atoms) and empty cubes [$\square Ni2_8$] parallel to the 4-fold axes, which are separated by Ni-centered cubooctahedra [$Ni1Ni3_{12}$]. This particular arrangement of metal clusters forms a superstructure which can be related to the $AuCu_3$ structure type. Boron atoms in the structures of binary borides crystallizing in the $CuAl_2$ type also have tetragonal antiprismatic coordination (e.g., Ni_2B) [12]. Lu resides at the center of a Friauf polyhedron formed by Ni atoms [$LuNi2_4Ni3_{12}$].

The electronic density of states (DOS) calculated for the ideal composition $Lu_2Ni_{21}B_6$ is dominated by Ni states at the Fermi level (E_F), where only Ni1 (at the center of the cubooctahedron [$Ni1Ni3_{12}$]) significantly contributes. Calculations in the LSDA approach reveal no significant polarization of the electrons. Only for the Ni1 species a small, but significant induced moment of ≈ 0.2 μ_B is calculated (with ≈ 0.03 μ_B for Ni2 and ≈ 0.05 μ_B for Ni3). This results in a predicted total moment

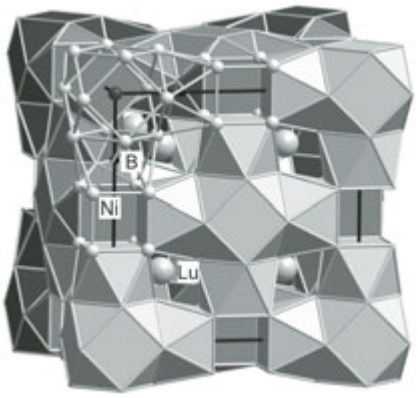

Fig. 1: Crystal structure of $Lu_{2-x}Ni_{21}B_6$.

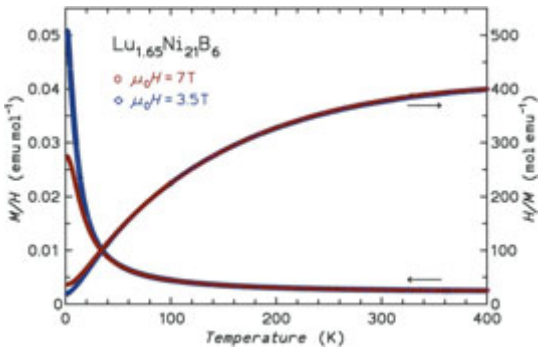

Fig. 2: Magnetic susceptibility of $Lu_{1.65}Ni_{21}B_6$.

of ≈ 1 μ_B/f.u. However, measurements of the magnetic susceptibility as a function of temperature $\chi(T)$ of a single phase sample (Fig. 2) gave no indication of ordered magnetism in $Lu_{1.65}Ni_{21}B_6$. $\chi(T)$ can be fitted by a modified Curie law $\chi(T) = \chi_0 + C/T$ including a rather large temperature independent contribution of $\chi_0 = 1.7\times10^{-3}$ emu/mol, and μ_{eff} = 1.5 μ_B/f.u. This is actually very close to the calculated ordered moment of ≈ 1 μ_B/f.u that corresponds to 1.73 μ_B/f.u for μ_{eff}.

Inspection of the partial DOS suggests that E_F can be shifted by hole doping (3.5 holes) into a region of enhanced partial Ni1 and Ni3 DOS (Fig. 3) resulting in an energy gain from magnetic exchange splitting in $Lu_2Ni_{21}B_6$.

Calculations were carried out in the virtual crystal approach (VCA) with all Ni sites doped equivalently. The results indicated increased moments of Ni1 (≈ 0.48 μ_B) and Ni3 (≈ 0.13 μ_B) but hardly any influence on the Ni2 (~ 0.02 μ_B) position. A total moment of ≈ 2.14 μ_B/f.u. is predicted. Indeed, upon substitution of Co for Ni in the compound $Lu_{1.62}Ni_{17.5}Co_{3.5}B_6$ a ferromagnetic ground state is experimentally observed with T_C = 71 K ≈ θ_P and a paramagnetic moment of μ_{eff} = 5.8 μ_B/f.u.

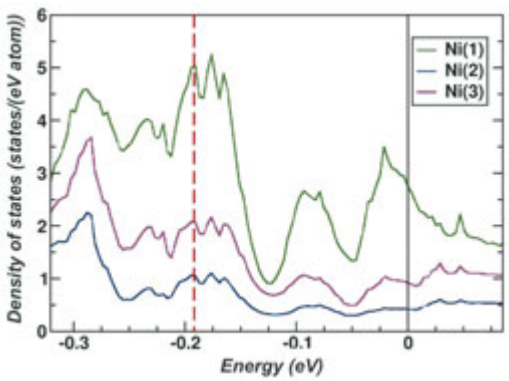

Fig. 3: Partial DOS of $Lu_2Ni_{21}B_6$.

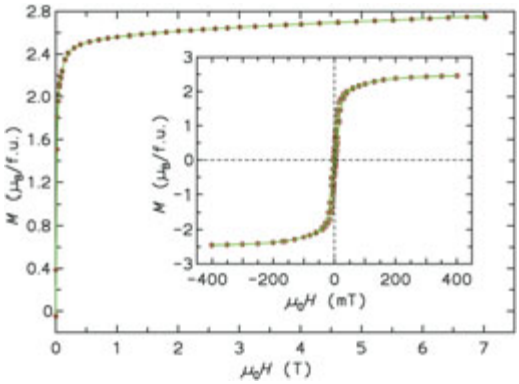

Fig. 4: Magnetization of $Lu_{1.62}Ni_{17.5}Co_{3.5}B_6$ at 1.8 K.

$Lu_{1.62}Ni_{17.5}Co_{3.5}B_6$ shows soft magnetic behavior with nearly no hysteresis (Fig. 4).

From the magnetization isotherm taken at 1.8 K a saturation magnetization of 2.5 μ_B/f.u. can be deduced which corresponds to a small moment of 0.12 μ_B per transition metal in this compound (compared with 0.61 μ_B and 1.72 μ_B in the elemental metals Ni and Co, respectively).

Chemistry and Physics of $EuPd_3B_x$

The binary non-magnetic compound $EuPd_3$ ($AuCu_3$ type of structure, space group $Pm\bar{3}m$) was found to exhibit a narrow range of homogeneity at 950°C. It can be best rationalized by the chemical composition Eu_xPd_{4-x} ($0.90 < x < 1.01$) with lattice parameter of the primitive unit cell a_P = 4.0800 Å at the Eu-rich and a_P = 4.1025 Å at the Pd-rich boundary. From WDXS analyses the homogeneity range of the binary phase can be described assuming a statistical mixture of excess Eu or Pd atoms on both crystallographic 1*(a)* and 3*(c)* sites of the cubic $AuCu_3$ prototype. The solubility of boron and its influence on the crystal structure has been studied by means of WDXS, X-ray powder diffraction, wet chemical analysis and theoretical methods. While the octahedral void at the center of the [□Pd_6] octahedron in $EuPd_3$ is empty, it gets gradually filled with boron in $EuPd_3B_x$, leading to the anti-perovskite arrangement type of the [BPd_6] framework in which the large electropositive Eu metal atoms are embedded (Fig. 8a).

Theoretical calculations based on the coherent potential approach (CPA) reveal that the 1*(b)* position at the octahedron center is indeed the most favorable one [9]. This results in a structure with significantly lower total energy compared to alter-

native positions as, e.g., 3*(d)* (suggested in literature) at the unit cell edge midpoints. With this experimental and theoretical initial information the focus has now been on the following interrelated issues: i) comparison of theoretical and experimental studies of the evolution of lattice dimension upon boron insertion and ii) assignment of the effect of europium valence transitions on the crystal structure. In Fig. 5 we show the calculated lattice parameter as a function of boron content in $RE Pd_3B_x$ (*RE* = Eu, Lu). $LuPd_3B_x$ was chosen as reference, since the 4*f* electron shell of Lu is full, so that in this case no particular behavior due the *f* electrons is expected. The lattice parameter smoothly increases, and its evolution is approximately linear within the range $0.3 < x < 1$, without saturation for high *x*. In contrast, calculations show a jump in Eu valence from Eu^{3+} to Eu^{2+} which is also reflected in the discontinuity of the lattice parameter.

From experimental investigations several important results have to be taken into account, i) only a limited solubility of boron is observed in $EuPd_3$, ii) the lattice expansion upon boron uptake displays a discontinuity, iii) the crystal structure is modified, and iv) the magnetic properties change dramatically. They all can be explained by the fact that boron insertion in the [□Pd_6] octahedron not only simply expands the lattice but also significantly influences the electronic structure. In Fig. 6 we compare the experimentally observed lattice expansion of $EuPd_3B_x$ and the reference system $GdPd_3B_x$ with boron content *x*. A change of slope for the Eu compound (at $x = 0.2$) is clearly discernable, while for the Gd compound the lattice parameter linearly increases up to a boron fraction limit $x \approx 0.45$.

The limit of boron solubility in $EuPd_3$ is reached close to $x = 0.55$. In case of $GdPd_3B_x$ we observed a simple expansion of the anti-perovskite type of structure and thus can deduce the mere lattice effect of boron on the $REPd_3$ structure. In contrast, in $EuPd_3B_x$ the slope increases at $x = 0.2$ compared to $GdPd_3B_x$ with $x > 0.2$. This hints to an additional mechanism at work connected with the electronic structure of Eu. It is well known that *RE* metals mostly favor a trivalent state in solids. However, Eu has also been found in divalent state or even in more complicated configurations such as mixed or intermediate valences. The valence of the *RE* metals depends therefore on the fine tuning between the energy of interaction between localized *f* electrons and the cohesive energy of more delocalized electrons participating in the conduction bands of the metal. An anomaly in the unit cell volume of the compound relative to the lanthanide contraction rule for trivalent ions (in our case Gd) often points to an unusual valence state. This change in valence of Eu as a function of boron has been studied theoretically. It also has a significant influence on the crystal lattice since the ionic radius of the Eu^{2+} species is larger than that of Eu^{3+} and thus, gives rise to a change in slope of the lattice parameter increase.

Our LSDA+*U* calculations clearly indicate a sudden increase of the unit cell volume at a boron fraction of $x = 0.2$ followed by smooth lattice expansion and thus, strongly point towards an atypical behavior of the $EuPd_3B_x$ model compound (see Fig. 5). It has to be kept in mind that the theoretical formalism applied here is based on the hypothesis of a homogeneous and unique valence for the *RE* metal and is not appropriate to deal with

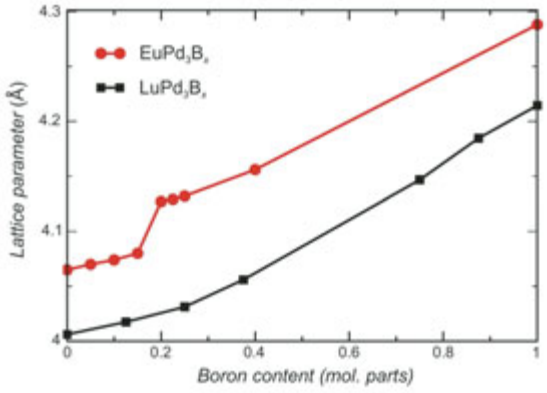

Fig. 5: Calculated lattice parameters of $REPd_3B_x$ (RE= Eu, Lu) as a function of boron content x.

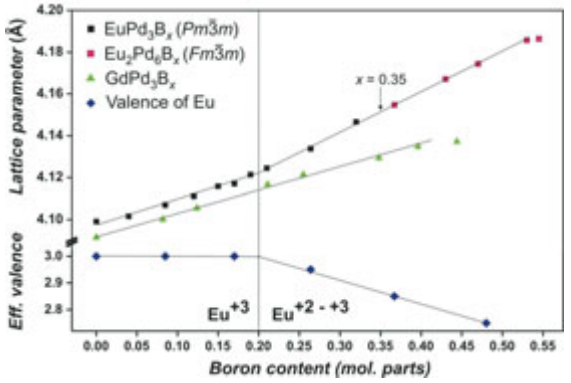

Fig. 6: Experimentally observed expansion of the primitive unit cell parameter a_P in $REPd_3B_x$ (RE = Eu, Gd) vs boron content x.

mixed or valence fluctuating states. Therefore, the calculations give us the most stable among different integer valence states. The fact that Eu adopts an unusual valence state in $EuPd_3B_x$ has also been observed experimentally by X-ray absorption spectroscopy (XAS) as can be seen in Fig. 7. There, the absorption spectra near the Eu L_{III} edge are presented. We perceive the dominant contribution of the $4f^6$ state (Eu^{3+}) and —depending on the boron fraction x— the gradual appearance of a second maximum on the low-energy side of the Eu L_{III} edge that indicates the contributions of $4f^7$ (Eu^{2+}) states. This is also reflected in magnetic susceptibility measurements. We observe Eu^{3+} with a nonmagnetic ground state $^7F_0$ in nominal $EuPd_3$, whereas the susceptibility strongly increases with boron contents $x > 0.26$ indicating an increasing Eu^{2+} ($^8S_{7/2}$) concentration.

Earlier Mössbauer effect investigations also indicated an unusual Eu valence in a sample with a nominal $EuPd_3B$ composition [13]. Samples prepared with this particular composition were found to contain significant amounts of the binary compound EuB_6.

Another remarkable phenomenon is related to the appearance of the divalent Eu, namely a subtle but significant modification of the crystal structure. Compounds with a boron content $x > 0.35$ crystallize with a supercell $2a_P \times 2a_P \times 2a_P$ (space group $Fm\bar{3}m$) with an ordered rock-salt-type arrangement of empty [$\square Pd_6$] and filled [BPd_6] octahedra. This situation is reminiscent of the crystal structure of ordered double perovskites $A_2MM'X_6$ where the ordering of octahedral-site cations M and M' doubles the unit cell of the simple, undistorted AMX_3 perovskite. Such a structural rearrangement can be rationalized in a chemical composition $Eu_2Pd_6B_x$ and gives rise to weak additional superlattice reflections in powder XRD and electron diffraction. The latter is shown in Fig. 8b. Interestingly, no such structural modification is observed for the $GdPd_3B_x$ compounds.

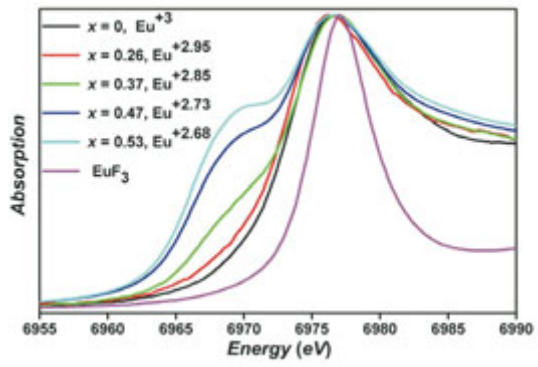

Fig. 7: Eu L_{III} XAS spectra of $EuPd_3B_x$ and effective valence of Eu atoms.

Determination of the Boron Content in Borides

Boron analyses and, more broadly, light element determination by microprobe WDXS is challenging due to the general issue that the measured intensities are related to the mass concentration. Also, the small energy of their X-ray lines gives rise to a strong influence of absorption effects. So, almost the complete detected intensity originates from the uppermost surface layer and, as a consequence, the intensity is strongly influenced by the quality of the local area that is probed by the electron beam. High-quality finishing during the metallographic preparation is recommended since also nano-surface layers may significantly alter the intensity. Additionally, it has been shown that energy and shape of the light-element X-ray lines are influenced significantly by the local environment and bonding situation of the light element. Thus, reference material and sample should be very similar in this respect.

The measurements (in a CAMECA SX 100 unit) on the $GdPd_3B_x$ and $EuPd_3B_x$ compounds were performed up to the maximal boron solubility (Fig. 6). This corresponds to a maximal content of approximately only 1 wt.% boron. For both systems the $REPd_3$ phase was used as standard material for the rare-earth element and Pd. The intensities of the *RE* Lα line (Eu Lα: 5846 eV; Gd Lα: 6057 eV) and the Pd Lα line (2839 eV) were measured. The monochromator crystals LPC3, LPET (Pentaerythritol, $d = 0.87$ nm) and LiF ($d = 0.4$ nm) were used for the B, Pd and *RE* lines. Pd_3B was used as standard for the B Kα line. The matrix correction model according to *Pouchou* and *Pichoir* [14] was applied to calculate the chemical composition. Different conditions have been applied for the measurement of the X-ray line of the heavy elements and boron. An acceleration voltage of 25 kV and a current of 20 nA results in count rates of ~ 10000 cps and 5000 cps for the Pd and the *RE* line, respectively. The boron line was measured by the area intensity method. Here, we applied 7 kV, 100 nA and a very long dwell time of 30 seconds

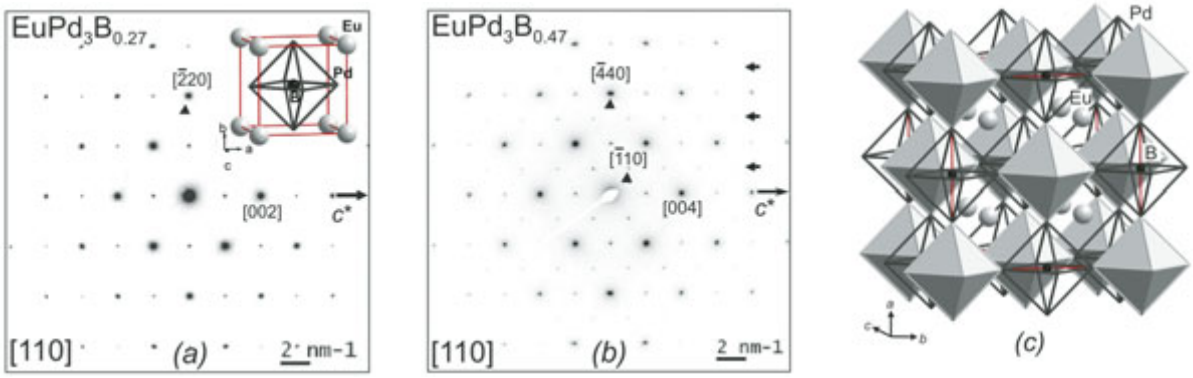

Fig. 8 (a) Crystal structure of $EuPd_3B_x$ and electron diffraction pattern for x = 0.27 and (b) x = 0.47. Arrows point to reflections indicating lattice parameter doubling. (c) Atomic arrangements in the Eu_2Pd_6B superstructure.

to master the small intensities. Additionally, the *RE*Pd_3 standards gave the possibility to determine the background intensity at the energy of the B *K*α line. As an example, the results of the samples with very small B content are given: $GdPd_3B_{0.08}$: Gd = 32.7(4) wt.% / Pd = 67.0(4) wt.% / B = 0.20(3) wt.%, analytical total Σ = 99.8 wt.%; $EuPd_3B_{0.09}$: Eu = 32.16(8) wt.% / Pd = 67.8(2) wt.% / B = 0.19(2) wt.%, analytical total Σ = 100.1 wt.%.

Both results agree well with the nominal boron content of 0.18 wt.% and 0.21 wt.% for $GdPd_3B_{0.08}$ and $EuPd_3B_{0.09}$, respectively.

Conclusion

Based on a concerted theoretical and experimental study of the two model systems $Lu_{2-x}Ni_{21}B_6$ and $EuPd_3B_x$ we demonstrate how electronic structure calculation combined with suitable experiments help to elucidate the underlying chemical physics. Motivated by the DOS at E_F of $Lu_2Ni_{21}B_6$ we were able to tune the magnetic properties by hole doping via Co substitution. A ferromagnetic ground state is observed for $Lu_{1.62}Ni_{17.5}Co_{3.5}B_6$ which shows soft magnetic behavior with nearly no hysteresis. For $EuPd_3B_x$ we observe Eu^{3+} with a non-magnetic ground state in nominal $EuPd_3$, whereas the susceptibility strongly increases with boron contents $x > 0.26$. The latter indicates an increasing Eu^{2+} concentration which is as well detected by Eu L_{III} XAS spectroscopy. LSDA+*U* calculations show a jump in Eu valence from Eu^{3+} to Eu^{2+} which is also reflected in the discontinuity of the calculated lattice parameter. Indeed, we can clearly discern a change of slope of the lattice parameter as a function of boron content *x* for the Eu compound (at $x = 0.2$). The boron content can be quantitatively determined by electron probe microanalysis of high-quality finished metallographic samples in combination with optimized reference compounds.

References

[1] *A. Westgren, G. Phragmen, and T. Negresco,* J. Iron Steel Inst. **117** (1928) 383.
[2] *A. Westgren,* Nature **132** (1933) 480.
[3] *F. R. Morral,* J. Iron Steel Inst., **130** (1934) 419.
[4] *H. H. Stadelmaier, in: B. C. Giessen (Ed.)*, Developments in the Structural Chemistry of Alloy Phases, Plenum Press, New York, London, 1969, pp. 141-181.
[5] *Yu. B. Kuzma and N. F. Chaban,* Binary and Ternary Systems Containing Boron, Handbook, Metallurgija, Moscow 1990 (in Russian).
[6] *L. Greer,* Science **267** (1995) 1947.
[7] *A. Inoue and A. Takeuchi,* Mater. Sci. Eng. A **375-377** (2004) 16.
[8] *I. Veremchuk et al.,* Solid State Sci., 11 (2009) 507.
[9] *C. Loison, A. Leithe-Jasper, and H. Rosner,* Physical Review B **75** (2007) 205135.
[10] *T. He et al.,* Nature 411 (2001) 54.
[11] *H. Rosner, R. Weht, M. D. Johannes, W. E. Pickett, and E. Tosatti*, Phys. Rev. Lett. **88** (2002) 027001.
[12] *P. Rogl, in J. J. Zuckermann (Ed.)*, Inorganic Reactions and Methods, Vol.13, 1991, pp. 85-167.
[13] *S. K. Dhar et al.,* Phys. Rev. B **29** (1984) 5953.
[14] *J. L. Pouchou, F. Pichoir, in: K. F. J. Heinrich, D. E. Newbury (Eds.)*, Electron probe quantitation. Plenum Press, New York, 1991, pp. 31-70.